DCIO2022
DESIGN COMPUTATION INPUT/OUTPUT CONFERENCE 2022.DOI:10.47330/DCIO.2022.ACSL3567

# A machine learning assisted preliminary design methodology for repetitive design features in complex structures

Omar A.I. Azeem[1], Lorenzo Iannucci.
Department of Aeronautics, Imperial College London, London, UK.
[1]oai15@ic.ac.uk, orcid.org/0000-0001-9849-5715

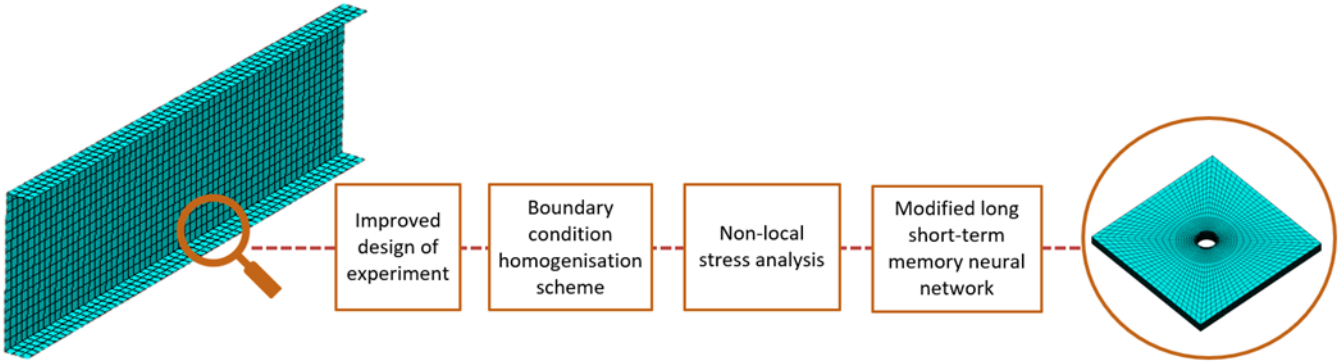


Fig. 1. Proposed computational methodology

## PART 1: PROPOSITION

**ABSTRACT.**

The current industrial practice used at the preliminary design stage of complex structures involves the use of multifidelity submodelling simulations to predict failure behaviour around geometric and structural design features of interest, such as bolts, fillets, and ply drops. A simplified global model without the design features is first run and the resulting displacement fields are transferred to multiple local models containing the design features of interest. The creation of these high-fidelity local feature models is highly expert dependent, and their subsequent simulation is highly time-consuming. These issues compound as these design features are typically repetitive in complex structures. This leads to long design and development cycles. Application of machine learning to this framework has the potential to capture a structural designer's modelling knowledge and quickly suggest improved design feature parameters, thereby addressing the current challenges.

In this work, we provide a proof of concept for a machine learning assisted preliminary design workflow, see Figure 1, whereby feature-specific surrogate models may be trained offline and used for faster and simpler design iterations. The key challenge is to maximise the prediction accuracy of failure metrics whilst managing the high dimensions required to represent design feature simulation parameters in a minimum training dataset size. These challenges are addressed using: a modified Latin Hypercube Sampling scheme adjusted to improve design of experiment in composite materials; a bi-linear work-equivalent homogenisation scheme to reduce the number of nodal degrees of freedom; a non-local volume-averaged stress-based approach to reduce the number of target features; and linear superposition of stacked bi-directional LSTM neural network models. This methodology is demonstrated in a case study of predicting the stresses of open hole composite laminates in an aerospace C-spar structure. Results highlight the high accuracy (>90%) and time saving benefit (>15x) of this new approach.

This methodology may be used to faster correct and iterate the preliminary design of any large or complex structure where there are repetitive localised design features that may contribute to failure, such as in Formula 1 or wind turbines. Combined with exascale computing this methodology may also be applied for predictive virtual testing of digital twins.

**KEYWORDS**

Machine learning, modelling, simulation, preliminary design

### 1. INTRODUCTION

Composite materials combine different materials to achieve superior properties. Commonly, they consist of a fibre component to carry mechanical loads, and a matrix component to transfer these loads to the fibres. The fibre-matrix components are manufactured commonly as plies where the fibre points in one direction. These plies are laid up in stacking sequences with plies facing varying angles to form a laminate. The overall properties of this laminate depend on the order of this ply sequence. This high tailorability of composite materials to suit application has resulted in the increasing adoption of composite materials in a variety of industries such as to build bridges, cars and planes. The recent Airbus A350 XWB and Boeing 787, for example, are over 50% composite material by volume, primarily carbon fibre- epoxy composite [BOEING 787, AIRBUS A350]. Carbon fibre-epoxy composite materials have high strength to weight and stiffness to weight ratios. Their

use can make structures more lightweight and so more environmentally friendly, especially structures whose carbon footprint is correlated with their weight, such as most transport vehicles. However, failure for such materials is multimodal, with failure possible by fibre tension, fibre split, fibre kinking and matrix cracking, for example [Pinho, Darvizeh, Robinson, Schuecker and Camanho. 2012]. This failure is driven by multiscale phenomena ranging from the microscale of reduced volume elements (RVEs) to the mesoscale of laminate layup and macroscale of structural components. Their complex, multiscale behaviour means that the computational failure modelling required to design and validate composite structures can be slow and expert dependent. In order to predict damage initiation, high-fidelity modelling is required, however modelling a large composite structure using high-fidelity techniques would be computationally unfeasible. To ease the computational burden of predicting failure within large structures, such as composite airframes, a one-way global-local finite element analysis is typically used at a preliminary design stage [Ostergaard, Ibbotson, Roux and Prior, 2011]. Figure 2 shows this current preliminary design methodology. The low-fidelity global model typically consists of a coarse 2D shell formulation to represent the macroscale structure; in aerospace, this may be an entire wing-box structure. Following the global analysis there is progressive local submodelling in areas of interest, which consists of higher fidelity modelling techniques such as solid 3D elements and higher mesh density to represent the small features of interest. These features of interest are typically design features such as bolts, fillets and ply-drops. Typically, this global-local modelling is displacement-based so the nodal displacements from the global model are used to drive the nodal displacements of the local model. Stress-based failure criteria such as LarC05 and Hashin are often used to predict the damage initiation indices. Typically, damage initiation is expected when these indices reach a value of 1, and multiple damage indices exist to represent different failure modes [Simulia, 2020].

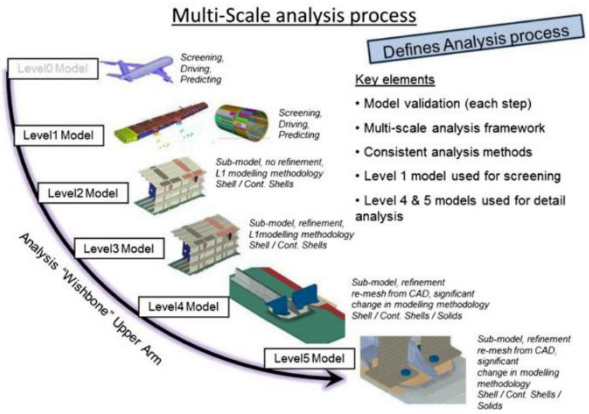


Fig. 2. Current preliminary design process for large composite structures [Ostergaard, Ibbotson, Roux and Prior, 2011]

However, this global-local modelling technique is still very expert-dependant and slow, especially as the local design features in composite structures are highly repetitive. These computational challenges lead to a slow design-development cycle which may reduce the added value of choosing these sustainable advanced materials over traditional metals. Therefore, this work aims to provide a proof of concept for a computational modelling technique that will lead to faster and less expert dependent preliminary design of large composite structures with repetitive features. To achieve this aim, we use machine learning techniques as they have demonstrated great success in the past of using offline expert-generated data to inform fast online predictions.

In this paper, we propose a machine learning-based computational methodology that can be used to predict damage initiation when varying the laminate stacking sequence, geometric design feature parameters and boundary conditions of a local design feature. The design feature in this proof of concept is a simple hole in plate, but the methodology is expected to be transferrable to more complex features such as bolts, fillets and ply drops, as long as the simulation remains linear elastic, as expected at a preliminary design phase. Faster failure predictions will also allow faster optimisation of features. The new workflow suggested for the structural analyst/ designer as well as the workflow to train our new design tool is depicted in Figure 3.

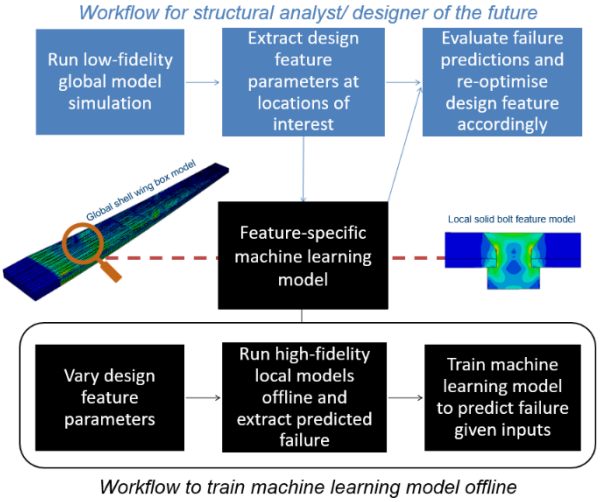


Fig. 3. Proposed preliminary design process for large composite structures

## 2. Literature Review

Machine learning has been used in literature for composite material failure predictions, but this has been towards predicting failure at a single scale (to predict the effect of skin-stringer geometry on buckling at a macroscale [Farokhi, Bacarreza, Ferri Aliabadi, 2020] and to predict stiffness of RVEs at a microscale [Liu et al., 2017], for example) or predicting multiscale failure that bridges micro-mesoscale via a constitutive law [Logarzo, Capuano, Rimoli, 2020], for example. However, there has been little research applying machine learning techniques to bridge the meso-macroscale which are the scales of concern in global-local submodelling at preliminary design stage. Also, the research to date either varies geometrical design feature parameters, laminate stacking sequence, or boundary conditions. There is no available research that has applied machine learning to predict failure when varying all three of these types of input features. Therefore, we are not yet able to quickly and easily predict the failure of custom local design features at variable global locations, as required for a global-local modelling framework.

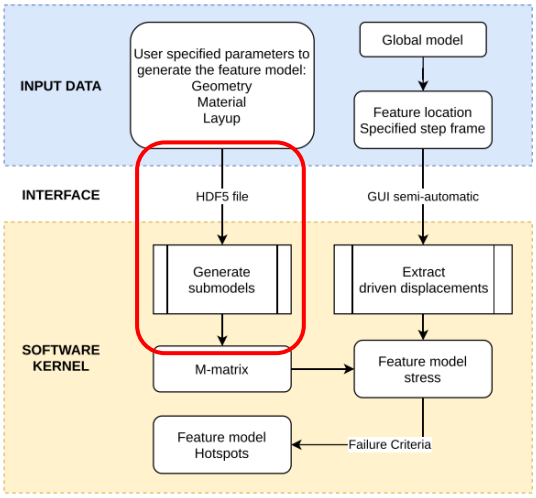


Fig. 4. General design for the workflow of an existing Abaqus plug-in, with the red highlighted area proposed to be replaced by a machine learning model [Zou et al, 2021]

There has been development effort to produce a simulation tool that performs analysis of repetitive features in large composite structures [Zou et al, 2021]. The general design for the workflow of this tool is shown in Figure 4, note that no machine learning is involved at any stage. This tool works by generating an M-matrix that stores the stress response of a given

local design feature, given a unit displacement applied to each nodal degree of freedom separately. The principal idea is that by saving this matrix, we are able to use the principle of linear superposition to superimpose the stress caused by the actual nodal displacements in the global model at the different locations that the local feature appears in. This is shown to result in satisfactory accuracy and high-time saving in the particular case where the exact same design feature occurs repetitively in a structure. However, this method is not flexible to a feature whose geometry or layup changes slightly, as an entirely new M-matrix would have to be generated every time. The shape of the M-matrix is defined as [*number of stress variants* x *number of integration points that stress is evaluated at* x *number of nodal degrees of freedom varied]*. The number of stress variants are six, the number of integration points that stress is evaluated at can be in the thousands depending on the local feature model and the number of nodal degrees of freedom can also be in the hundreds depending on the fidelity of the mesh. Therefore, calculating the M-matrix for each change in feature geometry or layup would be time-consuming. This leads to an opportunity to use machine learning to be able to predict the M-matrix, given a feature with variable layup stacking sequence and feature geometry. Further modifications are proposed to reduce the size of the M-matrix by reducing the nodal degrees of freedom (using bi-linear work-equivalent homogenisation) and reducing the number of integration points that stress is evaluated at (using a volume-averaged non-local approach).

## 3. Finite Element Modelling Methodology

Abaqus 2021 is used to develop the finite element models in this work. Both models are run as static, general simulations.

### *3.1. Global model*

The global model we use in this case study is a section of a C-spar typically used in composite airframes. We use a 0.125 mm thick T700/epoxy carbon fibre-epoxy prepreg to define the material properties, which are given in Table 1 [Qin et al. 2021]. The dimensions are sized based on the geometry of a small business jet and the quasi-isotropic layup is sized to satisfy a composite design guideline maximum of 4500 microstrains [Wang, Wan, Groh and Wang, 2021]. The layup used is $[45,\text{-}45,0,90]_{5s}$. The C-spar is modelled using coarse (10mm) shell elements as typically used in global airframe models. The dimensions and finite element modelling are depicted in Figure 5.

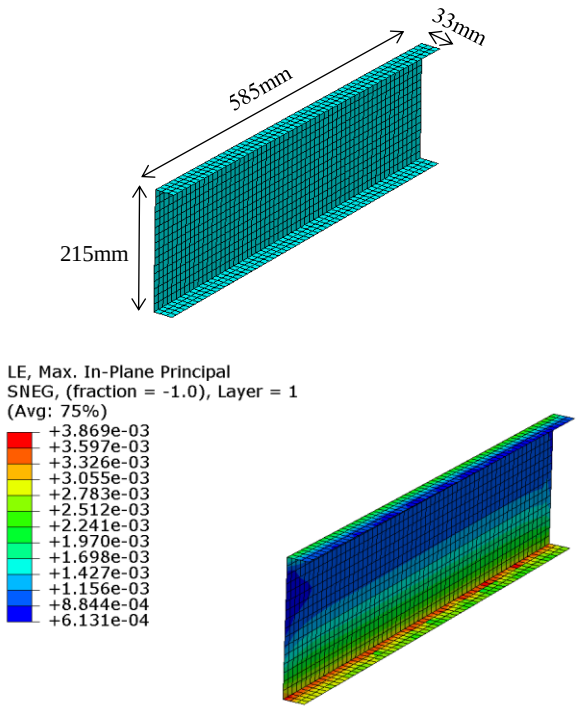


Fig. 5. Finite element modelling of global C-spar model. Dimensions and mesh shown in top and strain simulation results shown in bottom

TABLE 1. Material properties of carbon fibre-epoxy pre-preg [Qin et al. 2021]

| E11 (GPa) | E22 (GPa) | E33 (GPa) | v12 | v13 | v23 | G12 (GPa) | G13 (GPa) | G23 (GPa) |
|---|---|---|---|---|---|---|---|---|
| 125 | 8.4 | 8.4 | 0.3 | 0.3 | 0.4 | 4.2 | 4.2 | 3 |

### *3.2. Local model*

The hole in plate local model is modelled in a script which allows the hole diameter to be varied from 3mm to 8mm and the laminate stacking sequence to be explicitly specified. The thickness of our local models varies from 1mm to 10mm. The size of the local model is fixed as a 32mm square, so as to be able to fit within the C-spar flanges in the global-local modelling process. We use 3D solid elements for the finite element model, with one element per ply in the thickness direction. Further circular partitions are created through-thickness for the non-local approach described in Section 3.3. We use a structured hex mesh of size 1mm outside the circular partitions to 0.5mm within the circular partitions. Finer mesh size is applied towards the hole to improve the accuracy of the stress predictions in this area of interest. The dimensions and finite element modelling are depicted in Figure 6.

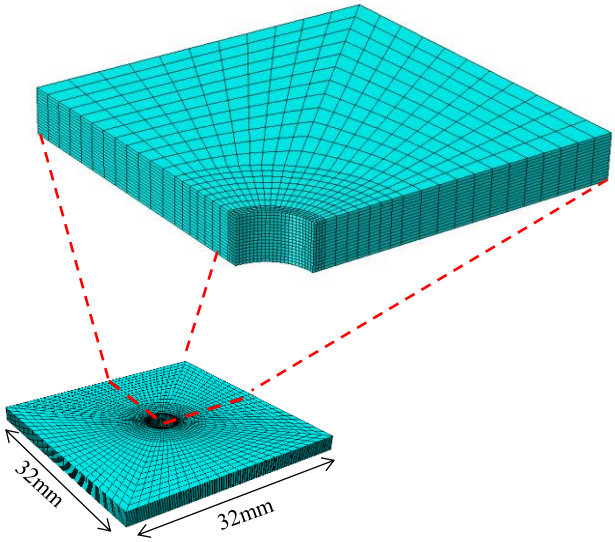


Fig. 6. Finite element modelling of local hole in plate model with magnified view to show meshing strategy

## 4. Machine Learning Modelling Methodology

R is used to generate the design of experiment and TensorFlow is used to generate the machine learning model in this work.

### *4.1. Design of Experiment – Modified Latin Hypercube Sampling*

The most commonly used type of composite laminates are classic quad laminates which are quasi-isotropic in nature, consisting of 0, 45,-45 and 90 degree plies. The variables in the design of experiment are thus the percentage of plies in each of these directions, as well as the total number of plies. These variables, as well as the geometrical design feature variable of hole diameter, are varied using a variant of the commonly used Latin Hypercube Sampling scheme, called Maximum Projection [Joseph, Gul and Ba, 2015]. This sampling scheme maximises the projection of each sampled point within the dimensions of the sampling space. We filter out unfeasible sampled points that violate the 10% rule [Niu, 1992], a common rule in the design of composite laminates which states that a feasible laminate must not contain less than 10% of any of the four quasi-isotropic ply angles.

The laminates generate in this work are restricted to symmetric, balanced laminates. To generate a specific layup stacking sequence, given the percentage of plies in each angle and the number of total plies, we implement an algorithm that follows further common design rules [Niu, 1992]. These design rules limit our laminates to having no more than 4 plies in a row that share the same ply angle and to laminates where the top and bottom plies are ±45 degrees for improved damage tolerance.

### *4.2. Input Feature Engineering – Bi-linear Work-equivalent Homogenisation of Boundary Conditions*

The local model may be located at arbitrary locations within the global model mesh. Furthermore, the mesh size of the global model may vary. To accurately determine the boundary conditions to transfer to the local model we implement an intermediate shell submodel of the same size as the local model but with a finer mesh size. Abaqus' in-built interpolation allows the boundary conditions to be transferred between these mesh sizes effectively. To reduce the number of nodal degrees of freedom, we implement an algorithm that recreates work due to displacement along each edge by applying displacements to only 4 corner nodes and 4 midside nodes. Thus, the net displacement along each edge, and so the net work, assuming that the stiffness is approximately constant along each edge, is conserved. The 8 boundary displacements in this homogenised intermediate submodel can then be used to drive the solid local feature model, in our case the hole in plate. Abaqus' shell-solid default submodelling procedure allows bending and plane rotation to be effectively captured. We thus have a fixed 24 degrees of freedom in total, as each node has 3 displacement degrees of freedom. To generate our M-matrix we only need to apply unit displacements to these 24 degrees of freedom. Figure 7 depicts the transition from global to local submodel via these extra intermediate submodels.

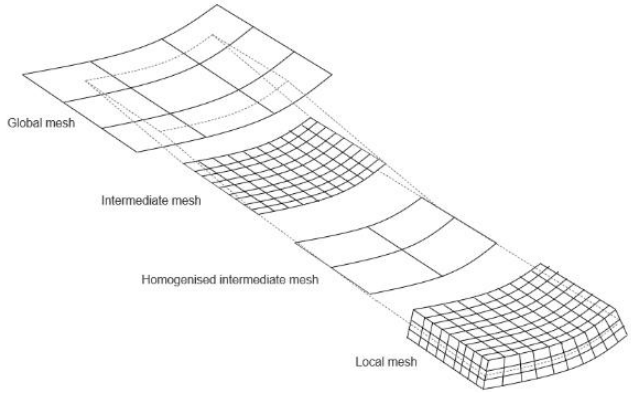


Fig. 7. Transition from global to local model via intermediate models

### *4.3. Output Feature Engineering – Non-local volume-averaged stress variants*

According to the principle of linear superposition, we can calculate the stress response due to a given set of boundary displacements by summing the stress response due to each boundary displacement individually. We are only concerned with the stress response in this work, as failure indices can be calculated at a later post-processing stage depending on the stress-based failure criterion chosen. It is unfeasible and unnecessary to predict the stress of each element in the local solid model using this linear superposition method, especially as the number of elements and location of elements will change between models. Likewise, the exact location of the maximum stress may change within a model depending on the model geometry. Therefore, we suggest determining the average stresses in a non-local area of interest. In our case we are most interested in the average stresses within 1.5 times the hole diameter, where the stresses are expected to be highest. We implement an algorithm that performs this non-local approach by volume averaging the 6 stress variants of the elements within this non-local area, per ply.

### *4.4. Machine Learning Network – Stacked Bi-Directional LSTMs*

Our input data for each local model is a sequence of ply layup angles and our output data is a M-matrix of volume averaged stresses with a size of [*number of stress variants* x *number of plies]*. We can split our output M-matrix to the 6 sequences for each stress variant. Therefore, our input and output shape are the same (that is the number of plies in the laminate), and our problem becomes a sequence-to-sequence problem. Predictive modelling of sequence-to-sequence problems are often tackled with sequential networks such as recurrent neural networks [Geron, A. 2019]. These networks feature a connection between the output of one block to the input of the next block and therefore the order of the sequence is considered. Long-short term memory neural networks are also a commonly used network that offer improvements over the basic recurrent neural network. These work by incorporating additional operations within each neuron block, that allows the network to selectively learn from elements which are further away from each other in the sequence. Figure 8 shows the structure of a basic RNN (top) featuring this feedback connection and a LSTM cell (bottom) featuring the additional operations.

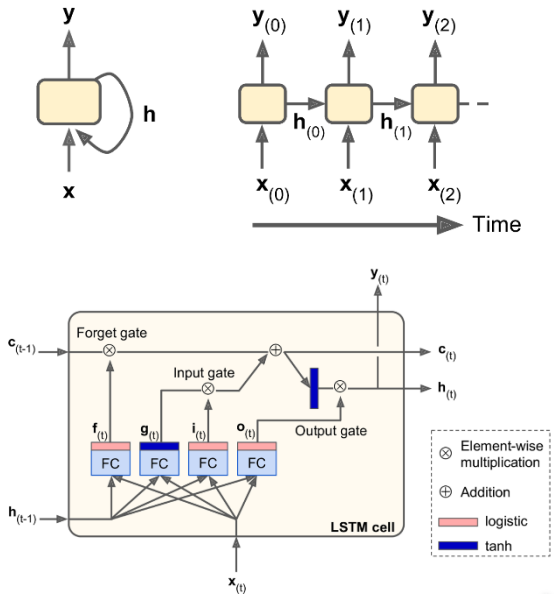


Fig. 8. Recurrent neural network block (top) and long short-term memory block (bottom) [Geron, A. 2019]

Both these neural networks can be stacked to increase their depth and so avoid overfitting to the training data. Bidirectionality can also be implemented for both these networks to allow predictions to consider the effect of elements of the sequence in both forward and backward directions. Our input data for each local model also includes a scalar indicating the local feature geometry, in our case the hole diameter. This can be added to our network as a separate feature for each laminate by creating a sequence that repeats this scalar by the length of the laminate stacking sequence. For all the networks the standard Adam optimiser is used, and they are run to 1000 epochs or until the network stops learning. Loss is calculated using mean squared error (MSE) and the error metrics are given as mean absolute error (MAE). Totally there are 133 samples generated, split into a training:validation:test ratio of 72:18:10.

## 5. RESULTS

In this work, we compare the performance of the LSTM over the RNN, and of further modifications such as stacking and bidirectionality, on the training and test accuracy of the local models. Furthermore, we use the best developed network to test the accuracy of our overall methodology in a global-local setting.

### 5.1. *Training*

The network architecture, a comparison of the training loss and validation loss as measured by Mean Squared Error (MSE), and sample predictions of stress against actual stress predicted by finite element analysis for degree of freedom 1 (DOF1) are shown in Figures 9-12 for each network investigated. Figure 13 shows the final validation error as measured by mean absolute error (MAE) for each network investigated.

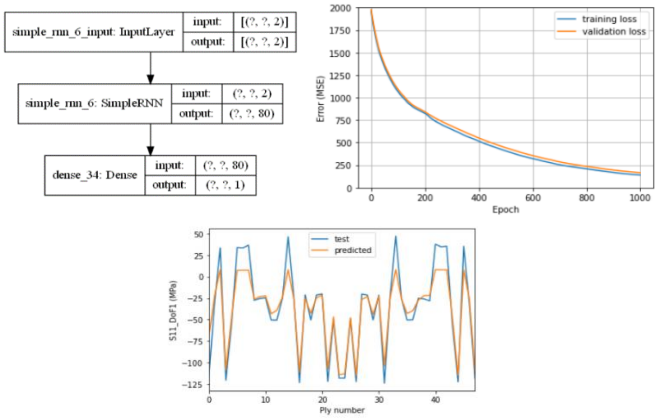


Fig. 9. RNN network: architecture (top left), training and validation loss diagram(top right), predicted S11 values for DoF1 (bottom).

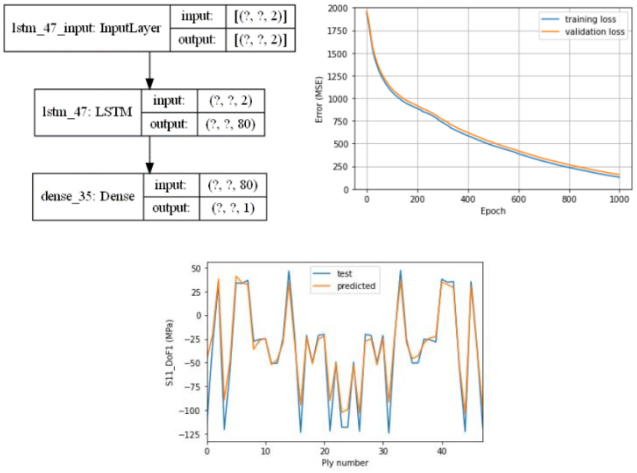


Fig. 10. LSTM network: architecture (top left), training and validation loss diagram(top right), predicted S11 values for DoF1 (bottom).

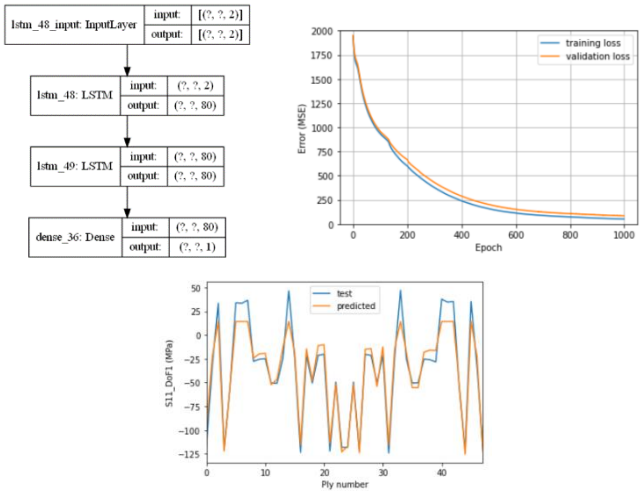


Fig. 11. Stacked LSTM network: architecture (top left), training and validation loss diagram(top right), predicted S11 values for DoF1 (bottom).

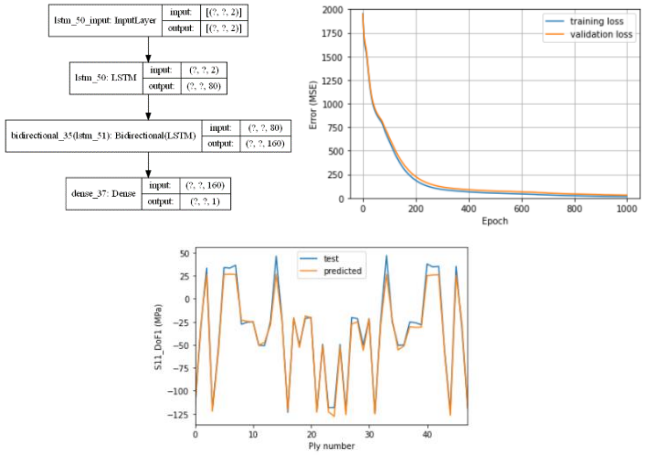


Fig. 12. Stacked bidirectional LSTM network: architecture (top left), training and validation loss diagram(top right), predicted S11 values for DoF1 (bottom).

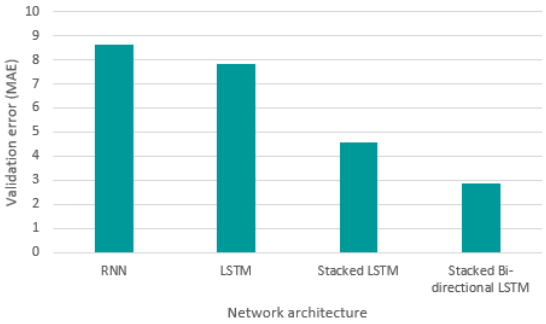


Fig. 13. Effect of network architecture on validation error

These results show that LSTM offers improvements over RNNs. This indicates that the effect of non-adjacent plies is important to determine the overall stress. This is reasonable as the laminate stiffness is commonly determined by consideration of all the ply angles, and this stiffness determines the stress faced by the laminate given a particular loading. Results also show that the stacked LSTM offers improvements over a regular LSTM. This indicates that the LSTM was slightly overfitting to the data when it was not stacked. Implementing bidirectionality also improves the accuracy of the LSTM, which is reasonable as the laminates under investigation are symmetrical, so reading the laminate forwards and backwards improves the predictions generated. The percentage error in predicted stresses across the test set laminates in the degree of freedom investigated is 5.03%. At a preliminary design stage this may be satisfactory. Especially as we are only concerned about errors in the largest stresses, where the errors are found to much lower.

### 5.2. *Testing overall methodology*

We validate our new machine learning based methodology by comparing stress predictions per ply against the stresses obtained through finite element submodelling. The stresses are queried for a given hole diameter (4mm) at four locations of the C-spar, see Figure 14, where bolt holes may exist for example. Results are satisfactory with the average percentage error in the peak stresses being 6.1%. This slight increase in error is associated with the boundary condition homogenisation method.

To interrogate the boundary conditions from the global model, run code to homogenise the boundary conditions, then predict failure using the machine learning model took ~2 minutes per hole analysed. Conversely, to generate a scripted 3d model in ABAQUS and run the submodelling simulation took ~30 minutes per sample. A scripted local model may not be available in such an analysis, therefore the time to generate finite element submodel may result in even greater time. More complex features such as bolts will take longer to model and simulate using the standard global-local methodology, whilst the time to run our

new methodology will be similar. Therefore, we have demonstrated a large (at least over 15x) time saving benefit of the new computational methodology.

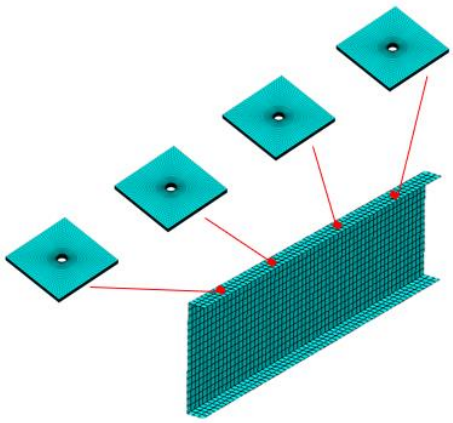

Fig. 14. Holes in C-spar case study to test developed methodology

## 6. CONCLUSION

In conclusion, we have demonstrated our new methodology to result in satisfactory stress predictions per ply given a local design feature of variable laminate stacking sequence and feature geometry under various boundary conditions. These stress predictions can be used to predict damage initiation at a preliminary design stage with failure criteria. We have also shown at least an order of magnitude time saving with this new methodology. This methodology may therefore be useful to accelerate the global-local preliminary design process commonly used for large composite structures with repetitive design features. This methodology, however, is not restricted to composite materials. The key techniques developed may be adjusted to faster simulate any complex feature which is repetitive in a structure, whether the complexity is due to material properties or feature geometry.

This methodology may be used in future to result in faster design optimisation and uncertainty quantification of failure. Combined with exascale computing and appropriate sensor placement, this methodology could also be applied for real-time predictive virtual testing of digital twins to predict damage initiation. Future work will involve proving this concept for a realistic local bolt feature applied to a large wing box global model. Further machine learning networks and techniques will be investigated.


PROCEEDING DOI: https://doi.org/10.47330/DCIO.2022.CAXL3310

# PART 2: IMPLEMENTATION [I/O SECTION]

### IMPLEMENTATION OVERVIEW

In this section we provide some input-output of the code used to (a) generate the design of experiment (b) perform the bi-linear work-equivalent homogenisation (c) derive the non-local stress variants (d) perform machine learning predictive modelling.

### (A) DESIGN OF EXPERIMENT

This code shows some code to generate the design of experiment using R and to modifications to then vary laminate stacking sequence

### INPUT

MaxPro code.

```
library("MaxPro")
x<-MaxProLHD(n = 200, p = 4)
X <- x$Design
Y <- X
Y[,1] <- X[,1]/rowSums(X[,1:3])
Y[,2] <- X[,2]/rowSums(X[,1:3])
Y[,3] <- X[,3]/rowSums(X[,1:3])
Y[,4] <- X[,4]
write.csv(Y,"~\\DoEMaxPro.csv", row.names
= FALSE)
```

Snippet of part of a function to modify design of experiment to vary laminate stacking sequence within design guidelines

```
num0=round(numpliessymm*portion0/100)
num45=myround(numpliessymm*portion45/100)
num90=numpliessymm-num0-num45
numpos45=num45/2
numneg45=num45/2
lyup=[]
lyup=45
numpos45-=1
options=[0,45,-45,90]
while num0+numpos45+numneg45+num90>0:
    option=random.choice(options)
    if option==45:
        if numpos45>0:
            lyup=np.append(lyup,option)
            numpos45-=1
            if numpos45==0:
                options.remove(45)
    elif option==-45:
        if numneg45>0:
            lyup=np.append(lyup,option)
            numneg45-=1
            if numneg45==0:
                options.remove(-45)
    elif option==0:
        if num0>0:
            lyup=np.append(lyup,option)
            num0-=1
            if num0==0:
                options.remove(0)
    else:
        if num90>0:
            lyup=np.append(lyup,option)
            num90-=1
            if num90==0:
                options.remove(90)
lyup=[lyup]

contiguityCheck=0
if lyup[0][-3]==lyup[0][-2] and lyup[0][-2]==lyup[0][-1]:
    contiguityCheck=1
for x in range(4,len(lyup[0])):
    if lyup[0][x]==lyup[0][x-1] and lyup[0][x]==lyup[0][x-2] and lyup[0][x]==lyup[0][x-3] and lyup[0][x]==lyup[0][x-4]:
        contiguityCheck=1
if contiguityCheck==0:
    lyups=np.append(lyups,lyup,axis=0)
```

### OUTPUT

This shows the samples chosen from the design of experiment, on a plot that shows the feasible region representing the 10% rule.

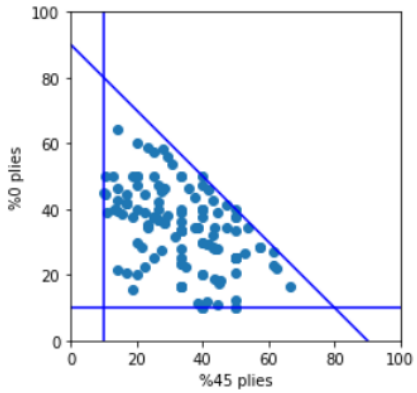


### (B) BI-LINEAR WORK-EQUIVALENT HOMOGENISATION

### INPUT

This code shows the main line of code that performs the homogenisation. The total area due to the high number of displacements along a given intermediate model edge is calculated, and a new midpoint displacement is suggested, that creates two triangles of an equivalent total area.

```
   array_newdisp[j]=[((1)*(array_disp[0,0]/2
+ sum(array_disp[1:-1,0]) + array_disp[-
1,0]/2))/(squaredim/2) -
0.5*(array_disp[0,0]+array_disp[-1,0]),
((1)*(array_disp[0,1]/2
```

### OUTPUT

This shows an example of the output array. Each row represents the x,y,z displacements of one of the 4 midside nodes along the boundary of the homogenised intermediate mesh.

```
array_newdisp
```

```
array([[-0.02140724, -0.03168382, -0.00947167],
       [ 0.00107174, -0.02576088, -0.00204317],
       [ 0.0175019 ,  0.01282067, -0.003066  ],
       [ 0.00494852,  0.03351765,  0.00489236]])
```

### (C) NON-LOCAL STRESS METHOD

### INPUT

This shows a code snippet of the function used to perform the non-local approach. By summing the volume and stress variants of the elements within the non-local area of each ply, we are able to calculate the volume averaged stress variants to use as target features for the neural network.

```
for ip in range(0,numElements):
      S11vsum = S11vsum + Stress[ip].data[0]*Volume[ip].data
      S22vsum = S22vsum + Stress[ip].data[1]*Volume[ip].data
      S33vsum = S33vsum + Stress[ip].data[2]*Volume[ip].data
      S12vsum = S12vsum + Stress[ip].data[3]*Volume[ip].data
      S13vsum = S13vsum + Stress[ip].data[4]*Volume[ip].data
      S23vsum = S23vsum + Stress[ip].data[5]*Volume[ip].data
      IVOLsum= IVOLsum + Volume[ip].data
S11avg = S11vsum/IVOLsum
S22avg = S22vsum/IVOLsum
S33avg = S33vsum/IVOLsum
S12avg = S12vsum/IVOLsum
S13avg = S13vsum/IVOLsum
S23avg = S23vsum/IVOLsum
outputs = [S11avg ,S22avg,S33avg,S12avg,S13avg,S23avg]
```


PROCEEDING DOI: https://doi.org/10.47330/DCIO.2022.CAXL3310

### OUTPUT

This shows some example results of the averaged stress variants per ply.

| | S11 | S22 | S33 | S12 | S13 | S23 |
|---|---|---|---|---|---|---|
| 2 | 0.143158 | 0.150046 | -0.00396 | 0.010273 | -0.00458 | 0.004844 |
| 3 | 0.972564 | 0.045714 | -0.00513 | -0.02277 | 0.066398 | 0.046231 |
| 4 | 0.641781 | 0.000684 | 0.005124 | -0.1222 | 0.152591 | 0.063395 |
| 5 | 0.36688 | -0.05609 | 0.000363 | -0.20482 | 0.243866 | 0.079993 |
| 6 | 0.105522 | -0.09224 | 0.000373 | -0.29187 | 0.329519 | 0.100626 |
| 7 | -6.54676 | 0.16337 | 0.00121 | -0.07091 | -0.38905 | 0.18537 |
| 8 | -0.43628 | -0.20035 | 0.003766 | -0.46064 | 0.478557 | 0.188346 |
| 9 | 5.76587 | -0.55909 | 0.004364 | 0.104162 | 0.211075 | 0.505803 |
| 10 | -11.5522 | 0.2395 | 0.004501 | -0.11476 | -0.47565 | 0.189983 |
| 11 | -4.66044 | -0.1488 | 0.004332 | 0.729242 | -0.24868 | 0.440636 |
| 12 | -5.36491 | -0.17716 | 0.003722 | 0.814894 | -0.38782 | 0.436081 |
| 13 | -16.6657 | 0.291502 | 0.007676 | -0.17002 | -0.50487 | -0.01943 |
| 14 | 9.577981 | -1.06557 | 0.008971 | 0.190173 | -0.04745 | 0.381777 |
| 15 | -1.94905 | -0.56606 | 0.006892 | -1.06049 | 0.238489 | 0.319025 |
| 16 | -22.065 | 0.359498 | 0.005176 | -0.21893 | -0.19839 | -0.03934 |
| 17 | -2.33252 | -0.68134 | 0.000486 | -1.25431 | -0.02025 | 0.016068 |
| 18 | -2.62656 | -0.76819 | -0.00381 | -1.35825 | 0.013148 | 0.001641 |
| 19 | -2.93758 | -0.8476 | -0.00537 | -1.44706 | 0.040728 | -0.01434 |
| 20 | -3.38709 | -0.9402 | -0.00451 | -1.5298 | 0.064776 | -0.03203 |

## (D) MACHINE LEARNING PREDICTIVE MODELLING

### INPUT

This shows a code snippet to generate and fit the machine learning network that achieved the best results in this work.

```
model = Sequential()
model.add((LSTM(80, return_sequences=True, input_shape=(None,2))),
model.add(Bidirectional(LSTM(80, return_sequences=True))),
model.add(Dense(1))
callback = tf.keras.callbacks.EarlyStopping(monitor='loss', patience=50, restore_best_weights=True)
model.compile(loss='mse', optimizer='Adam', metrics=['mae'])
history = model.fit(X_train,y_train,epochs=1000,callbacks=[callback], validation_split=0.2)
```

### OUTPUT

The training validation loss of this network is shown below

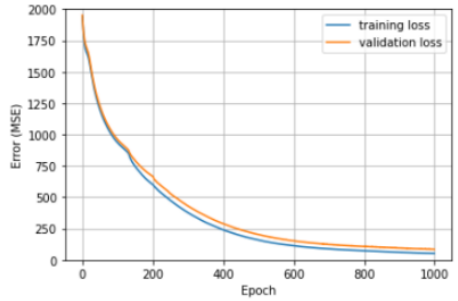



PROCEEDING DOI: https://doi.org/10.47330/DCIO.2022.CAXL3310

## REFERENCES


OSTERGAARD, M.G., IBBOTSON, A.R., ROUX, O.L., AND PRIOR, A.M. 2011. Virtual testing of aircraft structures. CEAS Aeronautical Journal 247, 1, 83.

BOEING 787. Article Title. Boeing 787 By Design Advanced Composite Use. https://www.boeing.com/commercial/787/by-design/#/advanced-composite-use

AIRBUS A350. Article Title. Airbus A350 Family. https://www.airbus.com/en/products-services/commercial-aircraft/passenger-aircraft/a350-family

PINHO, S.T., DARVIZEH R., ROBINSON P., SCHUECKER C. AND CAMANHO PP. 2012. Material and structural response of polymer-matrix fibre-reinforced composites. *Journal of Composite Materials*, 46(19-20)

SIMULIA. 2020. Article Title. Damage initiation for fibre-reinforced composites. https://help.3ds.com/2020/English/DSSIMULIA_Established/SIMACAEMATRefMap/simamat-c-

QIN, X., ET AL. 2021. Effects of countersunk hole geometry errors on the fatigue performance of CFRP bolted joints . Proc IMechE Part B: J Engineering Manufacture.

JOSEPH, V. R., GUL, E., AND BA, S. 2015. Maximum Projection Designs for Computer Experiments. Biometrika, 102, 371-380

damageinitfibercomposite.htm?contextscope=all&id=9291b1119c3345eba2858e79b982381f

FAROKHI, H., BACARREZA, O., FERRI ALIABADI, M.H., 2020. Probabilistic optimisation of mono-stringer composite stiffened panels in post-buckling regime. Structural and Multidisciplinary Optimization. 62:1395–1417

LIU, R., ET AL. 2017. Context Aware Machine Learning Approaches for Modeling Elastic Localization in Three-Dimensional Composite Microstructures. Integr Mater Manuf Innov 6:160–171

LOGARZO, H.J., CAPUANO, G., RIMOLI, J.J. 2020. Smart constitutive laws: Inelastic homogenization through machine learning. Computer Methods in Applied Mechanics and Engineering 373 113482

ZOU, X., ET AL. 2021. An Abaqus plugin for efficient damage initiation hotspot identification in large-scale composite structures with repeated features. Advances in Engineering Software 153 102964

WANG, Z., WAN, Z., GROH, R.M.J., AND WANG, X. 2021. Aeroelastic and local buckling optimisation of a variable-angle-tow composite wing-box structure. Composite Structures 258 11320

NIU MC-Y. 1992 Composite Airframe Structures: Practical Design Information and Data. Hong Kong: Conmilit.

GERON, A. (2019). Hands-on machine learning with Scikit-Learn, Keras and TensorFlow: concepts, tools, and techniques to build intelligent systems (2nd ed.). O'Reilly.


 PROCEEDING DOI: https://doi.org/10.47330/DCIO.2022.CAXL3310 